

Static and Dynamic Stereochemistry of *O*-Substituted *N*-9-Triptycylhydroxylamines

Gaku Yamamoto,* Chiharu Agawa, and Mao Minoura

Department of Chemistry, School of Science, Kitasato University, Kitasato, Sagami-hara, Kanagawa 228-8555

(Received November 8, 2002)

The static and dynamic stereochemistry of *N*-9-triptycylhydroxylamine derivatives (TpNHOR) with *O*-benzyl (**3**), *O*-ethyl (**4**), and *O*-phenyl (**5**) groups were studied. X-ray crystallographic analysis revealed that these compounds reside in a chiral conformation, with the Tp–N–O–R dihedral angle of 140–160°. Dynamic NMR studies of **3** and **4** show the presence of two separate stereomutation processes: chirality reversal (enantiomer interconversion) and rotation of the Tp–N bond with retaining the chirality, the latter having a lower energy barrier. Compound **5** gave solely information on the Tp–N rotation because of the lack of a probe for chirality reversal.

We recently reported static and dynamic stereochemistry of *N*-alkyl- and *N,O*-dialkyl derivatives of *N*-9-triptycylhydroxylamine (**1**), among which are **2a–2c** (Chart 1).¹ X-ray crystallographic analysis of **2c** revealed that the nitrogen atom is tetrahedral and the molecule adopts a chiral conformation. Dynamic NMR studies in solution showed that the stereomutation by which the chiral conformation enantiomerizes takes place rapidly at room temperature but slows down at low temperatures. The stereomutation was interpreted in terms of two rate processes: “R-passing” and “O-passing”, in which the alkyl group R or the oxy group OR' passes over a benzene ring of the 9-triptycyl (Tp) moiety. Either process is accompanied by inversion of the nitrogen atom (chirality reversal) and partial rotation of the N–O bond, but the energy barrier is mainly governed by the steric repulsion among the substituents around the N–O moiety rather than by the intrinsic barriers to the nitrogen inversion and the N–O bond rotation. Lineshape analysis of the temperature dependent ¹H NMR spectra afforded energy barriers to these processes, which amount to 46–59 kJ mol^{−1} depending on the compounds.¹

The compounds, the detailed dynamic stereochemistry of which was reported in Ref. 1, are confined to those which carry an alkyl group together with the Tp group at the nitrogen atom. In the present article, dynamic stereochemistry of several *O*-substituted derivatives, **3–5**, of *N*-9-triptycylhydroxylamine (**1**), which carry a hydrogen atom on the nitrogen, are reported. These compounds show somewhat different behavior in dynamic stereochemistry than the one observed in compounds **2** carrying an alkyl group at the nitrogen atom. A preliminary report on the *O*-phenyl

compound **5** has been published.²

Results and Discussion

Synthesis. The *O*-alkyl compounds **3** and **4** were prepared by *O*-deprotonation of *N*-9-triptycylhydroxylamine (**1**)³ with potassium *t*-butoxide, followed by alkylation with benzyl bromide and ethyl iodide, respectively.

The *O*-phenyl compound **5** was fortuitously obtained by the reaction of 9-nitrosotriptycene with phenyllithium, which we expected to afford *N*-phenyl-*N*-9-triptycylhydroxylamine.² The formation of **5** is ascribed to the single electron transfer (SET) from phenyllithium (PhLi) to 9-nitrosotriptycene (TpNO) to give two radical species (Ph• and TpNO•), followed by recombination of the two radicals and subsequent protonation.

X-ray Crystallography. Single crystals suitable for X-ray crystallography were obtained for all the compounds examined and were subjected to crystallographic analysis. The analysis was made at 100 K for **3** and **4** and at 23 °C for **5**. The perspective drawings of the molecular structures of **3** and **4** are shown in Fig. 1, while the one for **5** has been given in the preliminary report.² The representative bond lengths and angles are compiled in Table 1.

Although the positions of hydrogen atoms were not strictly optimized, the pyramidal nature of the nitrogen atom was confirmed for each of the compounds. The C1–N–O plane almost bisects the notch made by the two flanking benzene rings of the Tp moiety in each compound, conforming to the staggered conformation of the Tp–N bond. The nonplanarity of the C1–N–O–C5 moiety together with the pyramidal nature of the nitrogen atom give rise to the chiral nature of the molecules. The C1–N–O–C5 dihedral angles are 161°, 151°, and 143° for **3**, **4**, and **5**, respectively, considerably deviating from the “ideal” value of 120° that comes from the least electrostatic repulsion between the lone-pair electrons on N and O atoms.⁴ The deviations are mainly ascribed to the steric repulsion between the *O*-alkyl or *O*-phenyl group and the nearby perihydrogen of the Tp moiety (see Scheme 1), although the crystal packing forces may play some role.

Stereodynamics in Solution. ¹H NMR spectra of **3–5** at 23

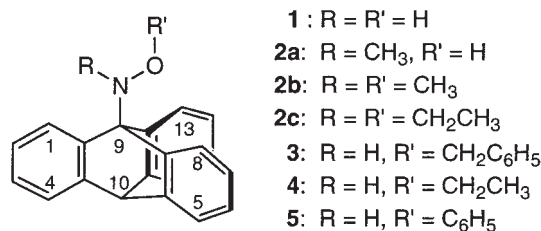


Chart 1.

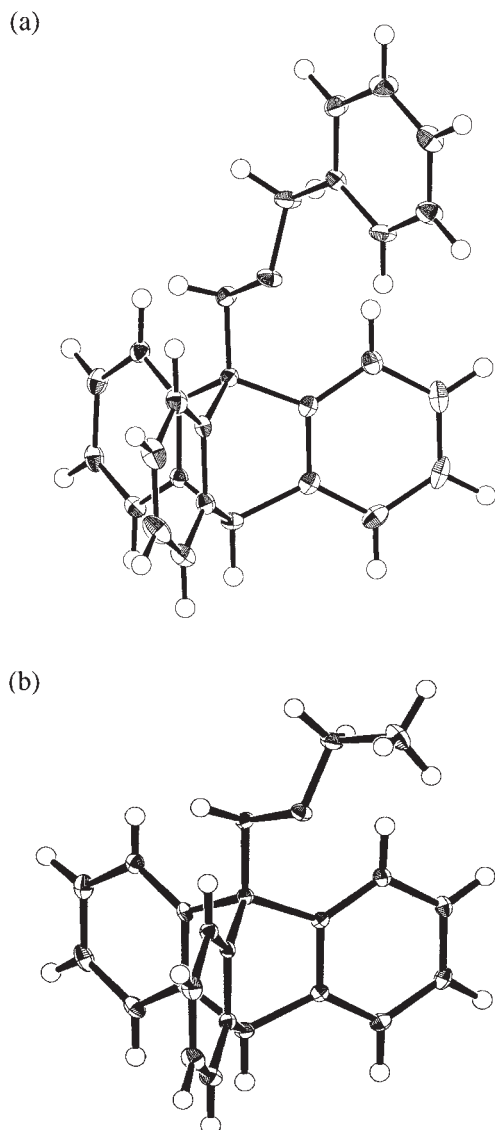
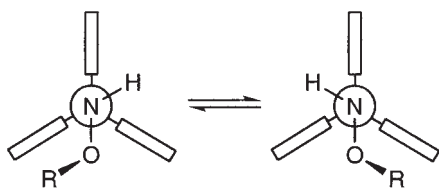


Fig. 1. Perspective drawings of the X-ray molecular structures of (a) compound **3** and (b) compound **4**.

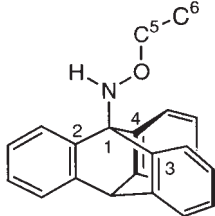


Scheme 1.

$^{\circ}\text{C}$ showed that all the stereomutation processes are rapid on the NMR timescale: three benzene rings of the 9-triptycyl (Tp) moiety are equivalent in each of compounds **3–5** and the methylene protons of the benzyl and the ethyl groups in **3** and **4**, respectively, are isochronous.

Upon lowering the temperature in, e.g., CD_2Cl_2 , the singlet signal of the methylene protons of **3** broadened, decoalesced at ca. -30°C , and appeared as an AB-type quartet at -90°C (Table 2). Similarly, the quartet methylene signal of **4** decoalesced at ca. -30°C into a complex spectrum ascribable to the AB part of an

Table 1. Selected Bond Lengths (\AA) and Angles ($^{\circ}$) for Compounds **3–5**



	3	4	5^{a)}
N–O	1.445(2)	1.458(2)	1.460(4)
N–C1	1.444(2)	1.461(2)	1.462(5)
O–C5	1.419(2)	1.434(2)	1.375(5)
C1–C2	1.526(2)	1.542(2)	1.555(3)
C1–C3	1.532(2)	1.539(2)	1.532(6)
C1–C4	1.535(2)	1.535(2)	1.530(5)
C5–C6	1.496(2)	1.511(2)	1.415(6)
O–N–C1	107.5(1)	106.1(1)	106.2(3)
N–O–C5	106.9(1)	108.4(1)	112.8(3)
N–C1–C2	109.4(1)	110.6(1)	108.6(3)
N–C1–C3	117.4(1)	116.6(1)	117.4(4)
N–C1–C4	113.2(1)	112.9(1)	114.1(3)
O–C5–C6	108.3(1)	107.6(1)	114.1(3)
C1–N–O–C5	161.0(1)	151.1(1)	143.3(3)
N–O–C5–C6	$-176.6(1)$	$-171.2(1)$	$-174.4(4)$
O–N–C1–C2	175.3(1)	177.4(1)	175.0(3)
O–N–C1–C3	55.1(2)	58.5(1)	56.2(4)
O–N–C1–C4	$-69.7(1)$	$-67.0(1)$	$-70.1(4)$

a) From Ref. 2.

Table 2. Chemical Shifts of the Methylene and *peri*-Proton Signals of **3**, **4** and **5** at ca. -90°C ^{a)}

Compd	Solvent	Methylene protons ^{b)}	<i>peri</i> -Protons
3	CD_2Cl_2	5.30, 5.18 (11.5)	7.75, 7.67, — ^{c)}
	$\text{C}_6\text{D}_5\text{CD}_3$	5.10, 4.81 (11.5)	7.98, 7.93, 7.05
	$(\text{CD}_3)_2\text{CO}$	5.37, 5.20 (10.6)	7.94, 7.81, 7.34
	CD_3OD	5.34, 5.16 (10.7)	7.87, 7.71, 7.26
4	CD_2Cl_2	4.28, 4.19 (8.9)	7.89, 7.52, 7.24
	$\text{C}_6\text{D}_5\text{CD}_3$	4.14, 3.79 (8.9)	7.98, 7.84, 7.22
	$(\text{CD}_3)_2\text{CO}$	4.25, 4.20 (8.9)	7.90, 7.56, 7.30
	CD_3OD	4.31, 4.22 (8.9)	7.88, 7.54, 7.26
5	CD_2Cl_2	—	7.97, 7.47, 7.28

a) Given in δ in reference with the solvent signal (CD_2Cl_2 : δ 5.32; $\text{C}_6\text{D}_5\text{CD}_3$: δ 2.09; $(\text{CD}_3)_2\text{CO}$: δ 2.04; CD_3OD , δ 3.30). b) Observed as an AB spin system for **3** and the AB part of an ABX₃ spin system for **4**. In parentheses are the geminal coupling constants in Hz. c) The third, highest-field signal is not identified due to the overlap with other aromatic signals.

ABX₃ spin system (Table 2). Nonequivalence of the methylene protons at low temperatures indicates that the molecules are frozen on the NMR timescale into a chiral conformation, as typically depicted in Scheme 1, and the temperature dependent lineshape change reflects the change in the rate of the chirality reversal, i.e., the interconversion between the enantiomeric conformers (Scheme 1). Full lineshape analysis gave the rate

Table 3. Kinetic Parameters for the Stereomutation Processes^{a)}

Compd	Solvent	Chirality reversal		Tp–N rotation		
		ΔG^\ddagger (250 K) ^{b)}	k (250 K)	ΔG^\ddagger (200 K) ^{b)}	k (200 K)	k (250 K)
		kJ mol ^{−1}	s ^{−1}	kJ mol ^{−1}	s ^{−1}	s ^{−1}
3	CD ₂ Cl ₂	50.3	160			
	C ₆ D ₅ CD ₃	49.8	210			
	(CD ₃) ₂ CO			42.3	37	9.6×10^3
	CD ₃ OD	50.8	130	42.9	26	7.8×10^3
4	CD ₂ Cl ₂	50.0	190	40.5	110	2.3×10^4
	C ₆ D ₅ CD ₃	49.5	240	39.0	270	3.7×10^4
	(CD ₃) ₂ CO	49.3	260	41.2	72	1.3×10^4
	CD ₃ OD	50.9	120	42.6	32	6.9×10^3
5	CD ₂ Cl ₂			45.6	5.0	1.2×10^3

a) Calculated from the ΔH^\ddagger and ΔS^\ddagger values given Table 4. b) Reliable to ± 0.4 kJ mol^{−1}.

constants for the process at several temperatures in the range of 20–30 °C, and the least squares analysis of the Eyring plots afforded the activation enthalpy and entropy values. The activation free-energies at 250 K were calculated by interpolation of these values and are compiled in Table 3. The ΔG^\ddagger (250 K) values range between 49 and 51 kJ mol^{−1} irrespective of the group R and the solvent. Compound **5** has no probe for the chirality reversal and thus gave no information on it.

The lineshapes of the aromatic protons of the Tp moiety in **3–5** also showed extensive dependence on the temperature. The signal ascribed to the peri-protons (1, 8, and 13-H) of the Tp moiety appeared as a single multiplet at 23 °C at the lowest field of the aromatic region of the ¹H NMR spectrum in any of compounds **3–5**, showing the equivalence of the three benzene rings of the Tp moiety. When the temperature was lowered, the signal broadened and decoalesced into three signals at ca. −70 °C for **3** and **4**, and at ca. −50 °C for **5**, indicating that the three benzene rings are mutually nonequivalent at low temperatures. This was confirmed by the ¹³C NMR spectra at ca. −100 °C, where nearly 18 different Tp aromatic carbon signals were recognized, although some were overlapped.

An important aspect here was that the lineshape change of the aromatic signals in **3** and **4** occurred at a lower temperature range than that of the methylene proton signals that is due to the chirality reversal, clearly indicating that the lineshape change of the aromatic signals reflects the “pure” rotation of the Tp–N bond with the retention of the chirality. This meant that the lineshape at a given temperature should be simulated in terms of a single rate constant. Actually the lineshapes of the peri-proton signals in compound **3–5** were successfully analyzed by using a single rate constant for a three-site exchange, though those for compound **3** in CD₂Cl₂ and toluene-*d*₈ could not be analyzed due to the extensive overlaps with the other aromatic proton signals. Again, the least-squares analysis of the rate constants at several temperatures afforded the activation enthalpies and entropies. The activation free-energies at 200 K and the rate constants at 200 and 250 K are given in Table 3. For compounds **3** and **4**, the ΔG^\ddagger values at 200 K vary in the range of 39–43 kJ mol^{−1}, and the rate constants for Tp–N rotation are ca. 10² times larger than those for chirality reversal at 250 K (Table 3). For compound **5** the free-energy barrier is ca. 5 kJ mol^{−1} higher than that for **4** in CD₂Cl₂, presumably because of the larger steric demand of the phenyl group than the ethyl group.

Observation of the energy barriers to “pure” rotation of the Tp–N bond is unprecedented, because the chirality reversal has always had a lower energy barrier than the Tp–N rotation with retention of chirality in all the 9-triptycylamine derivatives hitherto studied: *N,N*-dialkyl-9-triptycylamines⁵ and *N*-alkyl-*N*-9-triptycylhydroxylamines.¹

The interconversion between the enantiomeric forms (Scheme 1) involves the configurational inversion at the nitrogen atom and the partial rotation of the N–O bond, which would take place not simultaneously but consecutively.⁴ For simple alkyl-substituted hydroxylamines, it was controversial as to which of the two processes, nitrogen inversion and N–O bond rotation, is the rate-determining step, and it is now generally accepted that nitrogen inversion is rate-determining.⁴ For the present compounds, if we assume that the geometries in solution are very similar to those in crystal, the enantiomerization requires rotation of the N–O bond by 38, 58, and 73° for **3**, **4**, and **5**, respectively, judging from the C1–N–O–C5 dihedral angles given in Table 1. Since it is hard to assume that these small degrees of rotation have the energy barriers of ca. 40 kJ mol^{−1}, it will be reasonable that the inversion at the nitrogen atom is the rate-determining step; eclipsing of the N–H bond with one of the Tp-benzene ring will take place at the transition state of the N inversion, and will contribute to the high barriers.⁶

Table 3 shows that the solvent does not significantly affect the barriers to both the chirality reversal and the Tp–N rotation, and the barrier is slightly higher in methanol-*d*₄ than in other solvents for both processes.

It has been suggested⁷ that the barrier to nitrogen inversion in amines increases in hydroxylic solvents such as methanol because the hydrogen bonding of the solvent molecule with the amine nitrogen stabilizes the sp³ pyramidal ground state more effectively than the sp² planar transition state. The higher barrier to chirality reversal of **3** and **4** in methanol-*d*₄ than in other solvents can be explained in a similar manner.

The increase in the barrier to Tp–N rotation in methanol-*d*₄ is quite unprecedented and may be understood so that the hydrogen bonding of the solvent molecule with the nitrogen increases the effective bulkiness of the NHOR moiety.

Experimental

General. Melting points are not corrected. ¹H and ¹³C NMR spectra were obtained on a Bruker ARX-300 spectrometer operating

Table 4. Results of Lineshape Analysis

Compd	Process ^{a)}	Solvent	ΔH^\ddagger	ΔS^\ddagger	Temp Range ^{b)}	Pts ^{b)}
			kJ mol^{-1}	$\text{J mol}^{-1} \text{K}^{-1}$	$^\circ\text{C}$	
3	CR	CD_2Cl_2	51.0 ± 1.0	2.5 ± 4.1	−49 to −28	7
		$\text{C}_6\text{D}_5\text{CD}_3$	50.2 ± 5.1	1.9 ± 21.7	−47 to −27	6
		$(\text{CD}_3)_2\text{CO}^{\text{c)}$				
	Rot	CD_3OD	53.6 ± 2.5	11.3 ± 10.5	−47 to −29	5
		$\text{CD}_2\text{Cl}_2^{\text{c)}$				
		$\text{C}_6\text{D}_5\text{CD}_3^{\text{c)}$				
		$(\text{CD}_3)_2\text{CO}$	44.0 ± 1.7	10.4 ± 8.3	−83 to −59	6
		CD_3OD	45.7 ± 0.9	13.8 ± 4.1	−77 to −55	6
		CD_2Cl_2	51.1 ± 1.4	4.6 ± 6.2	−57 to −38	5
		$\text{C}_6\text{D}_5\text{CD}_3$	50.0 ± 1.0	2.0 ± 4.3	−54 to −27	8
4	CR	$(\text{CD}_3)_2\text{CO}$	50.5 ± 3.7	4.8 ± 16.5	−58 to −45	4
		CD_3OD	53.4 ± 3.5	9.9 ± 15.1	−50 to −33	5
		CD_2Cl_2	42.5 ± 1.3	10.1 ± 6.8	−94 to −77	6
		$\text{C}_6\text{D}_5\text{CD}_3$	39.2 ± 1.6	1.1 ± 8.4	−93 to −72	5
		$(\text{CD}_3)_2\text{CO}$	41.6 ± 4.9	1.8 ± 23.6	−76 to −57	5
		CD_3OD	42.9 ± 1.5	1.6 ± 7.4	−78 to −54	6
		CD_2Cl_2	43.6 ± 1.4	-10.0 ± 6.5	−70 to −34	5
	Rot					

a) CR denotes chirality reversal, and Rot denotes Tp–N rotation. b) The temperature range and the temperature points used in the lineshape analysis. c) Lineshape analysis could not be made.

at 300.1 MHz for ^1H and 75.4 MHz for ^{13}C , respectively. Proton chemical shifts were referenced with internal tetramethylsilane ($\delta_{\text{H}} = 0$), while ^{13}C chemical shifts with the solvent peaks: CDCl_3 ($\delta_{\text{C}} = 77.0$) and CD_2Cl_2 ($\delta_{\text{C}} = 53.8$). Letters p, s, t, and q given along with the ^{13}C chemical shifts denote primary, secondary, tertiary, and quaternary, respectively. In variable-temperature experiments, temperatures were calibrated using a methanol sample and are reliable to $\pm 1^\circ\text{C}$.

***O*-Benzyl-*N*-9-triptycylhydroxylamine (3).** To an ice-chilled solution of 500 mg (1.75 mmol) of *N*-9-triptycylhydroxylamine (**1**)³ in 100 mL of diethyl ether were added successively a solution of 500 mg (4.45 mmol) of potassium *t*-butoxide in 40 mL of diethyl ether and 1.0 mL (8.4 mmol) of benzyl bromide under argon, and the mixture was stirred for 10 min at 0°C and for 30 min at room temperature. The mixture was washed successively with water and brine, dried over MgSO_4 , and evaporated. Column chromatography (SiO_2 , benzene) followed by recrystallization from CH_2Cl_2 –hexane (1:3) afforded 375 mg (57%) of **3**, mp 212–213 $^\circ\text{C}$. Found: C, 86.30; H, 5.63; N, 3.75%. Calcd for $\text{C}_{27}\text{H}_{21}\text{NO}$: C, 86.37; H, 5.64; N, 3.73%. ^1H NMR (CDCl_3 , 23°C) δ 5.274 (2H, s), 5.334 (1H, s), 6.98–7.04 (6H, m), 7.115 (1H, s, NH), 7.34–7.37 (3H, m), 7.39–7.50 (3H, m, *m*- and *p*-H), 7.52–7.55 (3H, m), 7.62–7.65 (2H, m, *o*-H). ^{13}C NMR (CDCl_3 , 23°C) δ 53.65 (1C, t), 70.92 (1C, q), 76.77 (1C, s), 121.70 (3C, t), 123.19 (3C, t), 125.04 (3C, t), 125.23 (3C, t), 128.26 (1C, t), 128.64 (2C, t), 128.74 (2C, t), 137.31 (1C, q), 144.16 (3C, q), 145.21 (3C, q). ^{13}C NMR (CD_2Cl_2 , -102°C) δ 51.62 (1C, t), 69.86 (1C, q), 75.76 (1C, s), 119.02 (1C, t), 121.80 (1C, t), 122.02 (1C, t), 122.86 (1C, t), 122.90 (1C, t), 123.06 (1C, t), 124.28 (1C, t), 124.35 (1C, t), 124.53 (1C, t), 124.60 (2C, t), 124.86 (1C, t), 127.76 (1C, t), 128.15 (2C, t), 128.17 (2C, t), 136.20 (1C, q), 142.40 (1C, q), 142.50 (1C, q), 143.58 (1C, q), 143.74 (1C, q), 143.76 (1C, q), 144.72 (1C, q).

***O*-Ethyl-*N*-9-triptycylhydroxylamine (4).** To an ice-chilled solution of 150 mg (0.53 mmol) of *N*-9-triptycylhydroxylamine (**1**)³ in 20 mL of diethyl ether was added successively a solution of 117 mg (1.58 mmol) of potassium *t*-butoxide in 25 mL of diethyl ether and 1.5 mL (18.3 mmol) of ethyl iodide under argon, and the mixture was stirred for 10 min at 0°C and for 30 min at room temperature. The

Table 5. Crystal Data of Compounds **3** and **4** and Parameters for Data Collection, Structure Determination, and Refinement

Compound	3	4
Empirical formula	$\text{C}_{27}\text{H}_{21}\text{NO}$	$\text{C}_{22}\text{H}_{19}\text{NO}$
Formula weight	375.45	313.40
Crystal system	monoclinic	monoclinic
Space group	$P2_1/c$	$P2_1/a$
$a/\text{\AA}$	8.234(6)	8.966(4)
$b/\text{\AA}$	19.654(15)	13.143(5)
$c/\text{\AA}$	12.149(10)	14.339(6)
$\beta/^\circ$	104.574(12)	106.012(4)
$V/\text{\AA}^3$	1903(3)	1624(1)
Z	4	4
$D_c/\text{g cm}^{-3}$	1.311	1.244
$\mu(\text{Mo-K}\alpha)/\text{cm}^{-1}$	0.079	0.077
Temp/K	100	100
$2\theta_{\text{max}}/^\circ$	55	54.5
No. of reflections measured		
Total	4192	3574
Unique	2914	3074
No. of refinement variables	266	217
Final R ; R_w	0.0519; 0.1315	0.0463; 0.0936
GOF	0.836	1.557

$$R = \Sigma \|F_o\| - |F_c| / \Sigma |F_o|, R_w \text{ on } F^2.$$

mixture was washed successively with water and brine, dried over MgSO_4 , and evaporated. Column chromatography (SiO_2 , benzene) followed by recrystallization from CH_2Cl_2 –hexane (1:3) afforded 116 mg (70%) of **4**, mp 162–163 $^\circ\text{C}$. Found: C, 84.37; H, 6.10; N, 4.43%. Calcd for $\text{C}_{22}\text{H}_{19}\text{NO}$: C, 84.31; H, 6.11; N, 4.47%. ^1H NMR (CDCl_3 , 23°C) δ 1.444 (3H, t, $J = 7.1$ Hz), 4.308 (2H, q, $J = 7.1$ Hz), 5.338 (1H, s), 6.97–7.04 (6H, m), 7.116 (1H, s, NH), 7.34–7.37 (3H, m), 7.55–7.57 (3H, m). ^{13}C NMR (CDCl_3 , 23°C) δ 14.23 (1C, p), 53.66 (1C, t), 69.93 (1C, s), 70.76 (1C, q), 121.70 (3C, t), 123.18 (3C, t), 125.06 (3C, t), 125.20 (3C, t), 144.28 (3C, q), 145.26 (3C, q).

^{13}C NMR (CD_2Cl_2 , -103°C) δ 13.36 (1C, p), 51.54 (1C, t), 69.18 (1C, s), 69.62 (1C, q), 119.06 (1C, t), 121.56 (1C, t), 122.24 (1C, t), 122.72 (1C, t), 122.78 (1C, t), 123.01 (1C, t), 124.31 (1C, t), 124.36 (1C, t), 124.51 (3C, t), 124.84 (1C, t), 142.29 (1C, q), 142.55 (1C, q), 143.68 (2C, q), 143.81 (1C, q), 144.73 (1C, q).

O-Phenyl-N-9-triptycylhydroxylamine (5). To an ice-chilled solution of 500 mg (1.77 mmol) of 9-nitrosotriptycene³ in 50 mL of dry diethyl ether was slowly added 1.1 mL (2.0 mmol) of a ca. 1.8 M solution of phenyllithium in cyclohexane–diethyl ether (7:3), and the mixture was stirred for 2 h. After quenching with 20 mL of water, the mixture was extracted with diethyl ether. The combined ether layers were washed with water and brine, dried over MgSO_4 , and evaporated. Preparative TLC (SiO_2 , CH_2Cl_2 :hexane = 3:7) followed by recrystallization from CHCl_3 –hexane afforded 60 mg (9.4%) of **5**, mp 145–147 $^\circ\text{C}$. Found: C, 86.34; H, 5.34; N, 3.92%. Calcd for $\text{C}_{26}\text{H}_{19}\text{NO}$: C, 86.40; H, 5.30; N, 3.88%. ^1H NMR (CDCl_3 , 23°C) δ 5.387 (1H, s, 10-H), 6.98–7.05 (6H, m, 2,3,6,7,14,15-H), 7.094 (1H, m, *p*-H), 7.396 (3H, m, 4,5,16-H), 7.439 (2H, m, *o*-H), 7.48–7.60 (6H, m, *m*-H, NH, 1,8, 13-H). ^{13}C NMR (CDCl_3 , 23°C) δ 53.69 (1C, t), 71.13 (1C, q), 113.78 (2C, t), 121.61 (3C, t), 121.64 (1C, t), 123.34 (3C, t), 125.17 (3C, t), 125.44 (3C, t), 129.58 (2C, t), 143.84 (3C, q), 145.15 (3C, q), 160.55 (1C, q). IR (KBr) 3250 w, 1590 s, 1484 s, 1456 s, 1223 s, 744 cm^{-1} . ^{13}C NMR (CD_2Cl_2 , -90°C) δ 51.92 (1C, q), 70.19 (1C, t), 112.80 (2C, t), 119.48 (1C, t), 121.00 (1C, t), 121.57 (1C, t), 122.31 (1C, t), 123.04 (2C, t), 123.23 (1C, t), 124.51 (1C, t), 124.60 (1C, t), 124.64 (1C, t), 124.84 (1C, t), 124.97 (1C, t), 125.30 (1C, t), 129.21 (2C, t), 142.06 (1C, q), 142.31 (1C, q), 143.53 (1C, q), 143.82 (1C, q), 143.85 (1C, q), 144.91 (1C, q), 159.63 (1C, q).

Lineshape Analysis. Total lineshape analysis was performed by visual matching of experimental spectra with theoretical spectra computed on an NEC PC9821Xs personal computer equipped with a Mutoh PP-210 plotter using the DNMR3K program, a modified version of the DNMR3 program⁸ converted for use on personal computers by Dr. Hiroshi Kihara. The methylene proton signals were analyzed as an AB and an ABX_3 spin-system for **3** and **4**, respectively, and the peri-proton signals as an $(\text{ABC})_3$ -type 3-spin-3-site system by neglecting the 4, 5, and 16-H signals. Temperature dependences of chemical shift differences and T_2 values were properly taken into account.

The activation enthalpies and entropies obtained by the least-squares analysis of the Eyring plots are compiled in Table 4 together with the temperature range and points used for the Eyring plots.

X-ray Crystallography. Crystals of compounds **3** and **4** were

grown from dichloromethane–hexane. The crystal data and the parameters for data collection, structure determination and refinement are summarized in Table 5. Diffraction data were collected on a Rigaku AFC7R diffractometer and calculations were performed using the SHELXL97 program.⁹ The structures were solved by direct methods, followed by full-matrix least-squares refinement with all non-hydrogen atoms anisotropic and hydrogen atoms isotropic. Reflection data with $|I| > 2.0\sigma(I)$ were used. The function minimized was $\Sigma w(|F_o| - |F_c|)^2$, where $w = [\sigma^2(F_o)]^{-1}$.

Crystallographic data for compounds **3** and **4** have been deposited at the CCDC, 12 Union Road, Cambridge, CB2 1EZ, UK and copies can be obtained on request, free of charge, by quoting the publication citation and the deposition numbers 200612 and 200613, respectively.

References

- 1 G. Yamamoto, F. Nakajo, N. Endo, and Y. Mazaki, *Bull. Chem. Soc. Jpn.*, **74**, 1467 (2001).
- 2 G. Yamamoto, K. Kuwahara, and K. Inoue, *Chem. Lett.*, **1995**, 351.
- 3 W. Theilacker and K.-H. Beyer, *Chem. Ber.*, **94**, 2968 (1961).
- 4 a) M. Raban and D. Kost, in "Acyclic Organonitrogen Stereodynamics," ed by J. B. Lambert and Y. Takeuchi, VCH Publishers, New York (1992), Chap. 2. b) F. G. Riddell, *Tetrahedron*, **37**, 849 (1981). c) M. Raban and D. Kost, *Tetrahedron*, **40**, 3345 (1984).
- 5 G. Yamamoto, H. Higuchi, M. Yonebayashi, Y. Nabeta, and J. Ojima, *Tetrahedron*, **52**, 12409 (1996).
- 6 The reported barriers to enantiomer interconversion in simple alkyl-substituted hydroxylamines range among 42–54 kJ mol^{-1} , typically 44.7 kJ mol^{-1} for *N*-isopropyl-*O*-methylhydroxylamine in CD_3OD and 53.5 kJ mol^{-1} for *N*-isopropyl-*N,O*-dimethylhydroxylamine in CDCl_3 .^{4a} These data are, however, not systematic but fragmentary and the discussion by direct comparison with our present data does not seem to be meaningful.
- 7 See for example: T. Drakenberg and J. M. Lehn, *J. Chem. Soc., Perkin Trans. 2*, **1972**, 532.
- 8 D. A. Kleier and G. Binsch, QCPE Program No. 165.
- 9 G. M. Sheldrick, "Program for the Refinement of Crystal Structures," University of Göttingen, Germany (1997).